Flash-Photolysis Studies of the Photochemical Reactions of Silanes with Chromium Hexacarbonyl

Shulin Zhang,[†] Gerard R. Dobson,[‡] and Theodore L. Brown*,[†]

Contribution from the School of Chemical Sciences, University of Illinois, Urbana, Illinois 61801, and Department of Chemistry, University of North Texas, Denton, Texas 76203. Received March 4, 1991. Revised Manuscript Received May 24, 1991

Abstract: The photochemical reactions following flash photolysis of *n*-hexane solutions containing silanes and $Cr(CO)_6$ have been studied. The silane adducts vary widely in stability. The kinetics of silane elimination from $Cr(CO)_5$(silane) in hexane solutions under a CO atmosphere were investigated. For $HSiClMe_2$ and $HSiClPh_2$, two distinct first-order decay processes were observed, corresponding to elimination of H–Si- and Cl–Si-bonded adducts. Decay is faster for the Cl–Si form of bonding. The rates of elimination at 25 °C were measured for a series of 14 silanes differing widely in steric and electronic properties. The stabilities of the $Cr(CO)_5(H–SiR'R_2)$ adducts increase with increasing electron-donor character of the silane, the opposite order from that observed for $(\eta^5\text{-}C_5H_5)(CO)_2Mn$(silane) and other related systems. The reversal of order reflects the relatively greater importance of σ donation to the metal in bonding to the more electrophilic Cr metal center.

The reactions of metal carbonyl compounds with main-group-element hydrides have long been of interest. Chalk and Harrod first showed that dicobalt octacarbonyl was capable of catalyzing hydrosilation reactions[1] and proposed a mechanism that involved oxidative addition to Co following CO loss. Jetz and Graham were the first to prepare products of the photochemical reactions of silanes with transition-metal carbonyl compounds.[2] These complexes, of general formula $(\eta^5\text{-}C_5H_5)(OC)_2Mn(H)SiR_3$, have since become the most widely studied examples of the addition of silanes to a 16-electron metal center produced by dissociative loss of CO.[3] Analogous compounds, such as $(\eta^5\text{-}C_5H_5)(OC)_2Re(H)SiR_3$,[4] and $(\eta^6\text{-}C_6H_6)(OC)_2Cr(H)SiR_3$,[2,5,6] also have been studied.

The reactions of silanes with transition-metal carbonyl compounds are of interest because hydrosilation is a reaction of considerable importance. Beyond this, however, the reactions of silanes serve as readily studied analogues of C–H bond activation. There has thus been wide interest in achieving a better understanding of the factors that affect the stability and nature of the silane addition products.

The η^2 coordination of a silane to a metal center through the Si–H bond can be thought of in one extreme as a three-center, two-electron bond, I, and in the other as an oxidative addition, II.[3] The extent to which a given product of addition of a silane

I   II
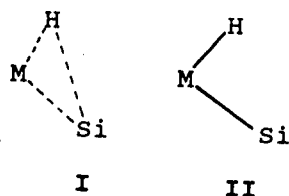
to a metal center corresponds to one or the other of these limiting cases can be discerned by using a variety of spectroscopic and structural probes. A wide range of bonding situations has been identified. In the $(\eta^5\text{-}C_5H_5)(OC)_2Mn(H)SiR_3$ series, the presence of electron-withdrawing species on the silicon atom, e.g., chlorine, results in stronger bonding to the metal center as compared with trialkylsilanes.[3,7] Concomitantly, the Si–H bond is relatively weaker; a variety of experimental probes, including NMR spectroscopy, X-ray structural determination, and valence photoelectron spectra, show that oxidative addition to the metal center is more advanced. The rationale for this trend is that the three-center bond between the Si–H bond and Mn comprises both donor and acceptor components. Bonding from metal 3d orbitals into the antibonding component of the Si–H bond, facilitated by electron-withdrawing groups on Si, shifts the electron distribution

toward that characteristic of Mn–H and Mn–Si bonds.

One measure of the stability of the bonding between the silane and metal center is found in the kinetics of dissociation of the silane. Hart-Davis and Graham studied the replacement of triphenylsilane from $(\eta^5\text{-}C_5H_5)(OC)_2Mn(H)SiR_3$ by ligands such as triphenylphosphine.[8] The reaction proved to be governed by rate-determining dissociation of the silane, with an enthalpy of activation of 29.2 kcal mol^{-1}. Activation parameters were determined by Schubert and co-workers for reductive elimination of $H–SiHPh_2$ from $(\eta^5\text{-}CH_3C_5H_4)Mn(CO)(PR_3)(H)SiHPh_2$, for various PR_3.[9] The activation enthalpy was found to increase with increasing electron density at the manganese atom.

An analogous sense of dependence on the structure of the silane is suggested also by the data for $(\eta^6\text{-}C_6H_6)(OC)_2Cr(H)SiR_3$ compounds.[5,6] In all these cases, the stabilities of the complexes are found to increase with increasing electron-withdrawing capacity of the groups attached to silicon.

Hill and Wrighton have reported the rates of addition of silanes to 16-electron metal centers at low temperature.[6] The activation parameters for addition to $(\eta^5\text{-}C_5H_5)Mn(CO)_2$ showed only small variations with silane. The barrier to addition presumably consists largely in the dissociation of solvent.

Although chromium hexacarbonyl has been shown to act as a photocatalyst for 1,4-hydrosilation of 1,3-dienes,[10] little is known about the properties of the intermediate formed by addition of a silane to $Cr(CO)_5$. Burkey recently produced the first evidence for adduct formation upon photolysis of a group VI metal hexacarbonyl with silanes such as $HSiEt_3$.[11] In addition to obtaining UV and IR spectroscopic evidence for adduct formation, he estimated the enthalpy of dissociation of the silane to be 21.1 kcal mol^{-1}, from photoacoustic calorimetry measurements.

Virtually nothing is known about the variation in energetics of binding to $Cr(CO)_5$ as a function of silane structure. The $Cr(CO)_5$ fragment differs from the $(\eta^5\text{-}C_5H_5)(OC)_2Mn$ fragment

---

[†] University of Illinois.
[‡] University of North Texas.

(1) (a) Chalk, A. J.; Harrod, J. F. *J. Am. Chem. Soc.* **1967**, *89*, 1640. (b) Harrod, J. F.; Chalk, A. J. *Organic Syntheses via Metal Carbonyls*; Wiley: New York, 1967; Vol. 2, pp 687–690.
(2) Jetz, W.; Graham, W. A. G. *Inorg. Chem.* **1971**, *10*, 4.
(3) Schubert, U. *Adv. Organomet. Chem.* **1990**, *30*, 151.
(4) Dong, P. F.; Hoyano, J. K.; Graham, W. A. G. *Can. J. Chem.* **1981**, *59*, 1455.
(5) Schubert, U.; Muller, J.; Alt, H. G. *Organometallics* **1987**, *6*, 469.
(6) Hill, R. H.; Wrighton, M. S. *Organometallics* **1987**, *6*, 632.
(7) (a) Lichtenberger, D. L.; Rai-Chaudhuri, A. *J. Am. Chem. Soc.* **1989**, *111*, 3583. (b) Lichtenberger, D. L.; Rai-Chaudhuri, A. *J. Am. Chem. Soc.* **1990**, *112*, 2492. (c) Lichtenberger, D. L.; Rai-Chaudhuri, A. *Inorg. Chem.* **1990**, *29*, 975.
(8) Hart-Davis, A. J.; Graham, W. A. G. *J. Am. Chem. Soc.* **1971**, *93*, 4388.
(9) Kraft, G.; Kalbas, C.; Schubert, U. *J. Organomet. Chem.* **1985**, *289*, 247–256.
(10) Wrighton, M. S.; Schroeder, M. A. *J. Am. Chem. Soc.* **1974**, *96*, 6235.
(11) Burkey, T. J. *J. Am. Chem. Soc.* **1990**, *112*, 8329.

in many ways, including the electron density at the metal center and steric requirements of the bound ligands. We have employed flash-photolysis methods to examine the kinetics of elimination of a series of 14 variously substituted silanes from $Cr(CO)_5$. The results are quite surprising; the order of stabilities of the bound silanes is the reverse of what one would predict for the $(\eta^5-C_5H_5)(OC)_2Mn(H)SiR_2$ and related series. Furthermore, the transient spectra reveal that hydridochlorosilanes can bind to the metal either through an H–Si or through a Cl–Si centered interaction.

Experimental Section

Materials. $Cr(CO)_6$ (Pressure Chemical Co.) was sublimed (30 °C, 0.3 mmHg) prior to use.

Carbon monoxide (Matheson Gas Products, Inc., Matheson purity grade, 99.99+%) was purged of $Fe(CO)_5$ by passage through a copper tube packed with activated charcoal heated to 180 °C in a sand bath followed by passage through a second charcoal-packed copper tube cooled in a dry ice–ethanol bath. The CO was then passed through a copper tube packed with activated 4A molecular sieves and an O_2 trap (American Scientific).

n-Hexane (Burdick and Jackson) was successively stirred with concentrated sulfuric acid for at least 7 days, washed with water several times, dried over anhydrous $CaCl_2$, passed through a column of freshly activated silica gel, refluxed over CaH_2, and distilled under Ar. It was then subjected to three freeze–pump–thaw cycles and stored in stoppered flasks in an Ar atmosphere glovebox.

$HSiEt_3$ (Aldrich Chemical Co.) was distilled over P_2O_5 under Ar. $HSiPh_3$ (ROC/RIC Research) was recrystallized from petroleum ether and dried under vacuum. $HSiCl_3$ (Aldrich Chemical Co.) was dried over 4A molecular sieves and distilled.

$HSiMePh_2$, H_2SiPh_2, $HSi(i-Pr)_3$, $HSiMe(C_6H_{11})_2$, $HSiMe_2(C_6F_5)$, $HSi(CH_2Ph)_3$, Me_3SiCl, $MeSiClPh_2$, and $MeSiCl_3$ were purchased from Aldrich Chemical Co. $HSiClMe_2$, $HSiClPh_2$, $HSiMe_2Ph$, and $HSiCl_2Ph$ were purchased from Lancaster Synthesis. These reagents were opened inside the Ar-atmosphere glovebox and used as received.

$HSiFPh_2$ was prepared from $HSiClPh_2$ and $(NH_4)_2SiF_6$ in 1,2-dimethoxyethane according to the previously reported method[12] and characterized by IR ($\nu_{Si-H} = 2169$ cm^{-1} in *n*-hexane) and mass spectrometry.

$HSi(C_6F_5)_3$ was prepared from $HSiCl_3$ and C_6F_5MgBr in diethyl ether according to procedures previously reported.[13] It was characterized by IR spectrometry ($\nu_{Si-H} = 2234$ cm^{-1} in *n*-hexane) and by melting point (134–136 °C) measurements.

Flash Photolysis. Samples for flash photolysis were loaded into cells fitted with threaded Teflon stopcocks. An attached Pyrex bulb (20–50 mL) was employed for mixing and freeze–pump-degassing of solutions. The cells used in the laser experiments were of quartz, with a 1-cm path length to both the laser photolyzing and the probe beams. The cells employed in the conventional (xenon-flash tube) flash-photolysis experiments were made of Pyrex glass with optical glass windows. The inner tube of the cells is 8 mm in diameter and 10 cm long along the probe-beam path. The cell temperatures were regulated to within 0.2 °C by circulating water from a constant-temperature bath through jacketed cells.

All the solutions were prepared in the glovebox. The solvent and liquid reagents were measured and transferred into the reaction cells by syringes. Solutions saturated with 1 atm of CO were first prepared in the glovebox and then subjected to freeze–pump-degassing for 20 min before exposure to 1 atm of CO while being stirred for 50 min at room temperature. The $Cr(CO)_6$ concentrations were in the range (1–2) × 10^{-4} M; at least a 20-fold excess of silane was employed to ensure pseudo-first-order reaction conditions.

The laser-flash-photolysis apparatus and data-acquisition system were described elsewhere.[14] In brief, the laser employed was normally an N_2 laser, emitting 337-nm radiation in pulses of about 10-ns width. Data were collected via a photomultiplier tube for determination of transient-signal behavior at a single wavelength or with an OSMA (Princeton Instruments, Inc.) photodiode array. The photodiode array afforded sampling through 512 channels in a 18-ns window of 300-nm width, in the wavelength range 400–700 nm, with a time resolution as short as 2 ns.

The conventional flash-photolysis apparatus, comprising two linear xenon-flash tubes and the associated detection system, has been described elsewhere.[14] Single-wavelength transient signals in the wavelength range 360–800 nm were collected by using a Hamamatsu 928 photomultiplier tube. The amplified signal was most commonly acquired by using a Markenrich WAAG board, which has 16 384 data points in a single channel, at acquisition rates varying from 20 MHz to 2 kHz. In a few cases, the rate processes observed were sufficiently slow that the 8-s maximum total data-acquisition time of the WAAG board was not sufficiently long. In these cases, the output voltages as a function of time were measured with a digital voltmeter.

Transient absorptions were observed and digitized by observing the probe beam at a wavelength in the range 360–550 nm. The wavelength of observation was normally chosen to optimize the signal-to-noise ratio for each individual reaction system. Kinetics data and UV–vis spectra were collected on floppy disks and later analyzed by employing self-developed ASYST-based computer programs and an AST 286 or Zenith 386SX microcomputer. The pseudo-first-order rate constants, k_{ob}, were calculated from traces obtained from a single flash in the conventional flash photolysis or from an average of 3–10 flashes in the laser-flash photolysis. In repetitive laser-flash experiments on a single solution, no significant variations in the calculated rate constants were noted. All rate constant data are presented with the value of one standard deviation given in parentheses.

Infrared spectra were recorded on a Perkin-Elmer Model 1710 FT-IR spectrometer, using a 1 mm path length cell with KCl windows. To obtain the IR spectra of photolyzed solutions, the IR cell was flashed by placing it between the xenon-flash tubes; it was then immediately moved to the IR spectrometer following the flash.

Results and Discussion

Formation of $Cr(CO)_5(HSiR_3)$ Complexes. The transient visible spectra obtained by employing a photodiode array apparatus following laser-flash photolysis of $Cr(CO)_6$ in hexane solutions in the presence of $HSiEt_3$ (10 mM) or $HSiCl_3$ (90 mM) are shown in Figure 1a,b, respectively. The species formed within 50 ns shows an absorbance maximum at about 510 nm. The absorbing species has been identified as the hexane-solvated complex $Cr(CO)_5$-(hexane).[15] Formation of the successor species in the presence of $HSiEt_3$, which takes place in the microsecond time domain, is evidenced from the growing absorbance with $\lambda_{max} \approx 400$ nm. This band, which decays on a time scale longer than milliseconds (vide infra), can be attributed to $Cr(CO)_5(HSiEt_3)$.[11] From the transient spectra in the range 400–650 nm of solutions containing $HSiCl_3$, the only evidence for formation of a second species accompanying the disappearance of $Cr(CO)_5$(hexane) is a slight increase in absorbance at 400 nm (Figure 1b). It is likely that the new species formed, presumably $Cr(CO)_5(HSiCl_3)$, absorbs at a shorter wavelength. To verify this assumption, conventional flash-photolysis experiments, which permitted a probe-beam wavelength as low as 360 nm, were performed at various monitoring wavelengths on a hexane solution of $Cr(CO)_6$ containing 59 mM $HSiCl_3$, and a point-by-point spectrum for the species generated within 200-μs after the flash was constructed. The spectrum obtained is shown in Figure 1c. From these results, it appears that $\lambda_{max} \leq 360$ nm for $Cr(CO)_5(HSiCl_3)$.

Kinetics of Solvent Displacement. The kinetics of hexane displacement by silanes from $Cr(CO)_5$(hexane) were studied by pulsed laser-flash-photolysis techniques. Plots of absorbance vs time following the flash of a hexane solution of $Cr(CO)_6$ containing 10 mM $HSiEt_3$, monitored at 540 and 420 nm, are shown in Figure 2a,b, respectively. The traces were fitted as exponential decay and growth, respectively; the insets display the corresponding linear plots of $\ln |A_t - A_\infty|$ vs time, where A_t and A_∞ are the absorbance at time t and final absorbance, respectively. The pseudo-first-order rate constants calculated from these two traces, which are direct indications of the consumption of $Cr(CO)_5$-(hexane) (at 540 nm) and the formation of $Cr(CO)_5(HSiEt_3)$ (at

(12) Damrauen, R.; Simon, R. A. *Organometallics* **1988**, *7*, 1161.
(13) (a) Schrieke, R. R.; West, B. O. *Aust. J. Chem.* **1969**, *22*, 49. (b) Eaborn, C.; Jenkins, I. D. *J. Organomet. Chem.* **1974**, *69*, 185.
(14) (a) Herrick, R. S.; Herrinton, T. R.; Walker, H. W.; Brown, T. L. *Organometallics* **1985**, *4*, 42. (b) Sullivan, R. S.; Brown, T. L. *J. Am. Chem. Soc.*, in press.

(15) (a) Welch, J. A.; Peters, K. S.; Vaida, V. *J. Phys. Chem.* **1982**, *86*, 1941. (b) Simon, J. D.; Peters, K. S. *Chem. Phys. Lett.* **1983**, *98*, 53. (c) Simon, J. D.; Xie. *J. Phys. Chem.* **1986**, *90*, 6751. (d) Simon, J. D.; Xie. *J. Phys. Chem.* **1987**, *91*, 5538. (e) Wang, L.; Zhu, X.; Spears, K. G. *J. Am. Chem. Soc.* **1988**, *110*, 8695. (f) Wang, L.; Zhu, X.; Spears, K. G. *J. Phys. Chem.* **1989**, *93*, 2. (g) Simon, J. D.; Xie. *J. Phys. Chem.* **1989**, *93*, 291. (h) Joly, A. G.; Nelson, K. A. *J. Phys. Chem.* **1989**, *93*, 2876.
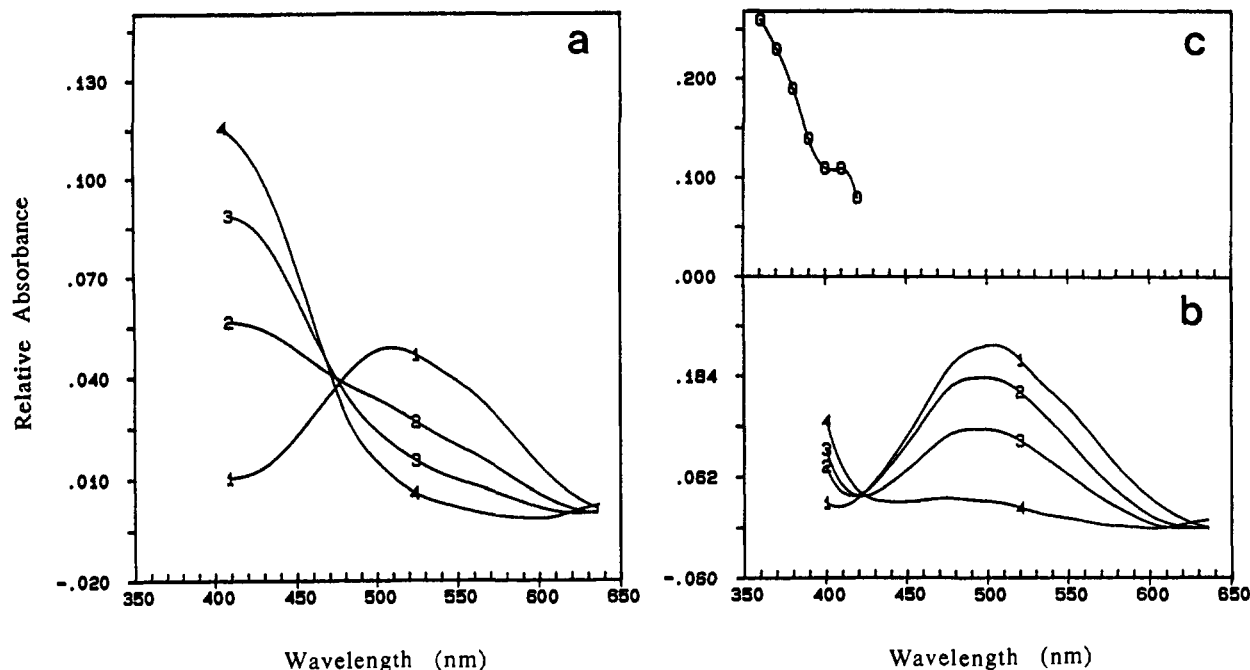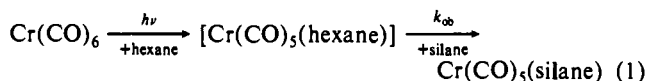
Wavelength (nm)   Wavelength (nm)

Figure 1. Transient visible spectra: (a) after laser-flash photolysis of a $Cr(CO)_6/HSiEt_3$/hexane ([$HSiEt_3$] = 10 mM) solution at times 2×10^{-8} (1), 5×10^{-6} (2), 8×10^{-6} (3), and 1×10^{-4} s (4); (b) after laser-flash photolysis of a $Cr(CO)_6/HSiCl_3$/hexane ([$HSiCl_3$] = 90 mM) solution at times 5×10^{-8} (1), 1×10^{-6} (2), 3×10^{-6} (3), and 2×10^{-5} s (4); (c) after xenon-flash photolysis of a $Cr(CO)_6/HSiCl_3$/hexane ([$HSiCl_3$] = 59 mM) solution within 200 μs of the flash.

Table I. Rate Constants of Reactions Observed after Laser-Flash Photolysis of $Cr(CO)_6$ in Hexane in the Presence of $HSiEt_3$ and $HSiCl_3$ at 21 °C

silane	[silane], mM	$10^{-5}k_{ob}$, s^{-1}	k, M^{-1} s^{-1}
$HSiEt_3$	8.54	1.14 (0.05)	1.33 (0.04) $\times 10^7$
	10.0	1.23 (0.02)	
	28.4	4.01 (0.05)	
	48.4	6.32 (0.08)	
	66.7	8.45 (0.73)	
	91.1	12.4 (0.3)	
$HSiCl_3$	19.8	0.39 (0.06)	1.54 (0.03) $\times 10^6$
	39.5	0.71 (0.01)	
	68.9	1.1 (0.2)	
	89.0	1.5 (0.3)	
	104.0	1.8 (0.4)	

420 nm), were found to have identical values within experimental uncertainty, 1.2×10^5 s^{-1}. This result is consistent with the fact that there is a fairly good isosbestic point in the time-resolved visible spectra. The reaction sequence is shown in eq 1.

$$Cr(CO)_6 \xrightarrow[+\text{hexane}]{h\nu} [Cr(CO)_5(\text{hexane})] \xrightarrow[+\text{silane}]{k_{ob}}$$
$$Cr(CO)_5(\text{silane}) \quad (1)$$

The rate constants of the solvent displacement were obtained at various silane concentrations. Table I lists these values from flash photolysis of $Cr(CO)_6/HSiR_3$/hexane (R = Et, Cl) solutions. The graphs of k_{ob} vs [$HSiR_3$], shown in Figure 3, indicate that the reaction is first order in silane concentration; i.e., $k_{ob} = k$-[$HSiR_3$].

As demonstrated by previous studies,[16] the displacement of solvent by nucleophiles from $Cr(CO)_5$(solvent) can take place via an interchange (I_d) pathway, a dissociative (D) pathway, or competitive interchange and dissociative pathways. Under the reaction conditions employed here, [hexane] $\gg$ [silane], these mechanisms are kinetically indistinguishable. However, both steric

(16) (a) Yang, G. K.; Vaida, V.; Peters, K. S. *Polyhedron* **1988**, *7*, 1619. (b) Zhang, S.; Dobson, G. R. *Inorg. Chim. Acta* **1989**, *165*, 11. (c) Dobson, G. R.; Zhang, S. *J. Coord. Chem.* **1990**, *21*, 155. (d) Zhang, S.; Dobson, G. R.; Zang, V.; Bajaj, H. C.; van Eldik, R. *Inorg. Chem.* **1990**, *29*, 3477. (e) Zhang, S.; Zang, V.; Bajaj, H. C.; Dobson, G. R.; van Eldik, R. *J. Organomet. Chem.* **1990**, *397*, 279.
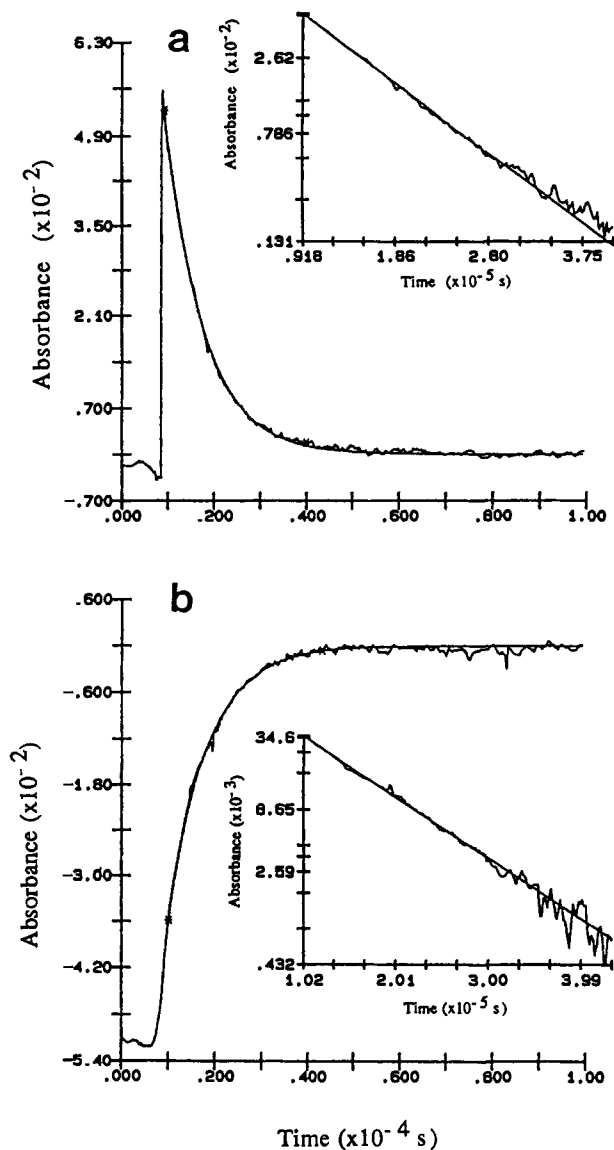
and electronic properties of the nucleophiles affect the mechanisms and rates of solvent displacement. Thus, although $HSiCl_3$ should be, if anything, less sterically demanding than $HSiEt_3$, the observed second-order rate constant is nearly 1 order of magnitude smaller for $HSiCl_3$ than for $HSiEt_3$. This difference in rates arises either because there is a small degree of bond making in the transition state for solvent displacement or because the less nucleophilic chloride competes less efficiently for $Cr(CO)_5$ following complete solvent dissociation.

Formation of the $Cr(CO)_5(HSiEt_3)$ complex is also evidenced in IR spectra recorded after 10 xenon tube flashes on a 2 mM hexane solution of $Cr(CO)_6$ containing 0.8 M $HSiEt_3$. Figure 4 shows the IR spectra of the solution before the flashes and at varying times thereafter. The two new peaks at 1952 (s) and 1940 (w) cm^{-1} observed after the flashes disappear over about 60 min, and the absorption due to $Cr(CO)_6$ (ν_{CO} = 1987 cm^{-1}) recovers its original intensity. This is consistent with replacement of silane by CO, eq 2.

$$Cr(CO)_5(\text{silane}) + CO \rightarrow Cr(CO)_6 + \text{silane} \quad (2)$$
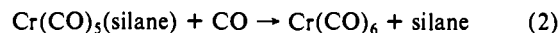
Analogous IR experiments were also performed for a solution containing 0.9 M $HSiPh_3$. A comparatively low intensity absorption at 1954 cm^{-1}, observed shortly after the flashes, disappears within 10 min. For the analogous solution containing 0.9 M $HSiCl_3$, no significant change in the IR spectrum was observed after xenon lamp flashes. These results indicate that elimination of $HSiPh_3$ from $Cr(CO)_5$ is faster than for $HSiEt_3$ and that elimination is still faster for $HSiCl_3$. The detailed kinetics of these elimination processes are elucidated in the flash-photolysis studies described below.

The Silane Elimination Reactions. The kinetics of silane elimination from $Cr(CO)_5$(silane) were investigated by employing a conventional xenon-flash-photolysis apparatus. The reactions occurred on a much slower time scale as compared with the hexane displacement processes. The slowest elimination process, that for $HSiEt_3$, takes place in minutes in the absence of added CO. A plot of absorbance vs time following the flash, monitored at 420 nm, for a hexane solution of $Cr(CO)_6$ containing 10.0 mM $HSiEt_3$ under Ar is shown in Figure 5a. The data are consistent with a second-order reaction, as shown by the linearity of the (absorbance)$^{-1}$ vs time plot shown in the inset. When the solution is saturated with 1 atm of CO, ([CO] $\approx$ 13.5 mM),[17] the rate

Photochemical Reactions of Silanes with Cr(CO)₆

J. Am. Chem. Soc., Vol. 113, No. 18, 1991 6911

Figure 2. Absorbance vs time following the flash of a $Cr(CO)_6$/$HSiEt_3$/hexane ([$HSiEt_3$] = 10 mM) solution, monitored at 540 nm (a) and at 420 nm (b). The traces were fitted as exponential decay and growth, respectively; the insets display the corresponding plots of ln $|A_t - A_\infty|$ vs time.
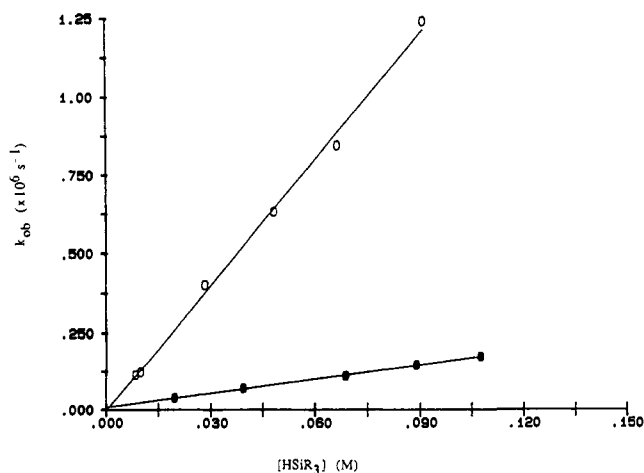

Figure 3. Plots of k_{ob} vs [$HSiR_3$] for hexane-displacement reactions at 21 °C. R = Et (open symbols), Cl (closed symbols).

is greatly increased, and the reaction obeys pseudo-first-order kinetics. Figure 5b and its inset show plots of absorbance vs time

Wavenumbers
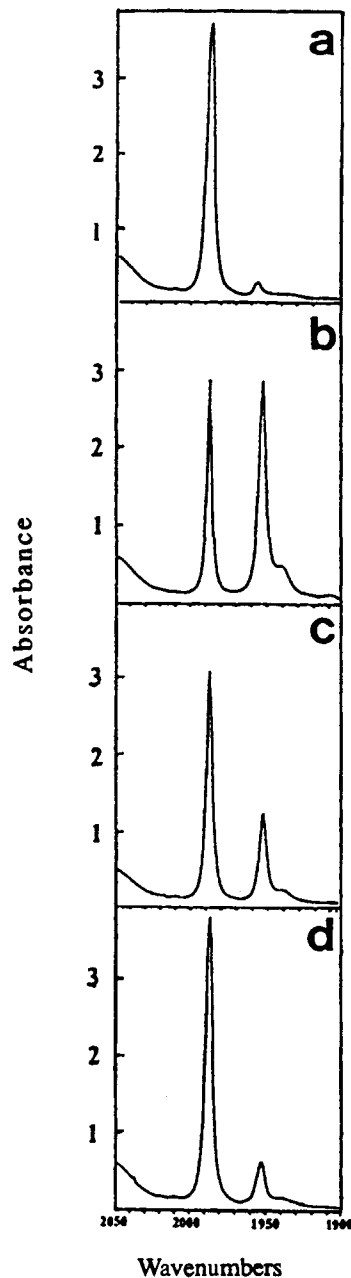
Figure 4. IR spectra of a $Cr(CO)_6$/$HSiEt_3$/hexane ([$Cr(CO)_6$] = 2 mM, [$HSiEt_3$] = 0.8 M) solution: (a) initial spectrum; (b) spectrum 1–2 min after 10 xenon tube flashes; (c) spectrum 12 min after the flashes; (d) spectrum 55 min after the flashes.

and of ln $(A_t - A_\infty)$ vs time, respectively. These results are consistent with silane substitution by CO to re-form $Cr(CO)_6$ as described in eq 2.

To probe the mechanism of silane elimination further, flash photolyses of $Cr(CO)_6$/$HSiEt_3$/hexane solutions under 1 atm of CO, with various $HSiEt_3$ concentrations, were carried out. As expected, the rate constants of the reaction decrease as [$HSiEt_3$] increases. The relationship is nonlinear; neither a plot of k_{ob} vs [$HSiEt_3$] nor a plot of k_{ob} vs [$HSiEt_3$]$^{-1}$ is linear for [$HSiEt_3$] in the 4–20 mM range. However, plots of $1/k_{ob}$ vs [$HSiEt_3$] are linear, as shown in Figure 6. This indicates that the reaction obeys a rate law of the form given in eq 3, which can be rearranged to eq 4.

$$k_{ob} = \frac{1}{a + b[HSiEt_3]} \qquad (3)$$

$$1/k_{ob} = a + b[HSiEt_3] \qquad (4)$$

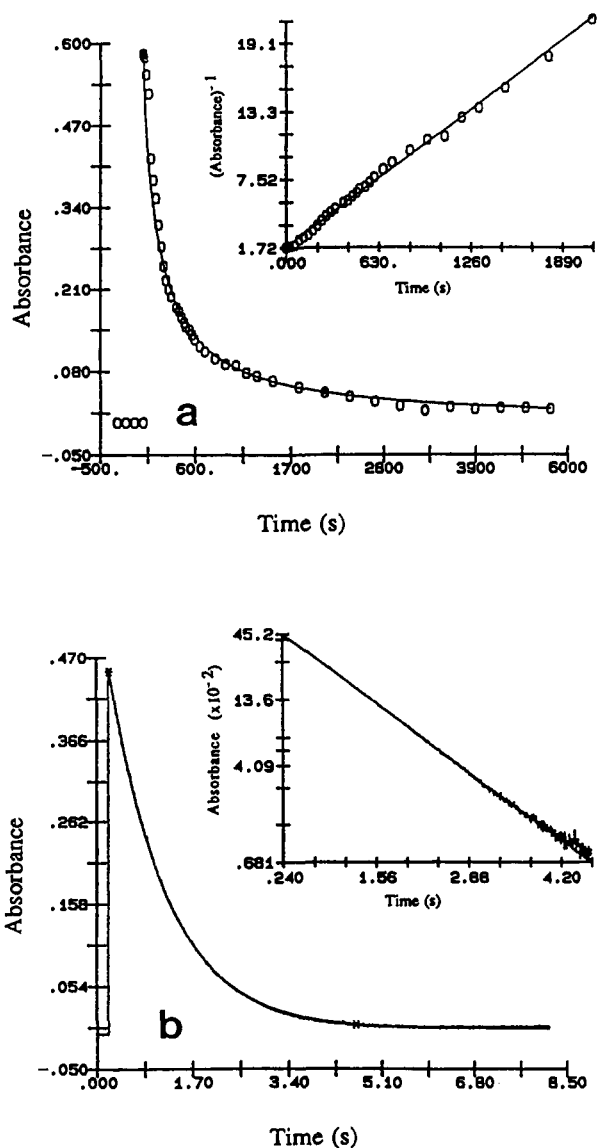(17) *Carbon Monoxide*; Cargill, R. W., Ed.; Solubility Data Series, Pergamon Press: New York, 1990; pp 51–52.

Time (s)

Table II. Rate Constants Involved in Silane Elimination Processes Observed from Flash Photolysis of $Cr(CO)_6$ in Hexane in the Presence of $HSiEt_3$ and $HSiPh_3$ at Various Temperatures under 1 atm of CO

silane	temp, °C	k_d, s^{-1}	k_{CO}/k_{Si}
$HSiEt_3{}^a$	13.2	0.64 (0.07)	0.47 (0.08)
	18.8	1.4 (0.1)	0.38 (0.05)
	25.0	2.6 (0.2)	0.41 (0.04)
	31.8	5.6 (0.3)	0.40 (0.03)
	39.6	14.5 (1.9)	0.29 (0.05)
$HSiPh_3{}^b$	13.2	34 (4)	0.32 (0.06)
	18.6	68 (8)	0.29 (0.04)
	25.0	143 (9)	0.26 (0.02)
	32.0	211 (24)	0.37 (0.06)
	40.0	485 (30)	0.32 (0.03)

$^a\Delta H^\ddagger{}_d = 20.0$ (0.5) kcal mol^{-1}; $\Delta S^\ddagger{}_d = +11$ (2) cal deg^{-1} mol^{-1}; $\Delta H^\ddagger{}_{CO} - \Delta H^\ddagger{}_{Si} = 2$ (1) kcal mol^{-1}; $\Delta S^\ddagger{}_{CO} - \Delta S^\ddagger{}_{Si} = -10$ (4) cal deg^{-1} mol^{-1}. $^b\Delta H^\ddagger{}_d = 16.4$ (0.9) kcal mol^{-1}; $\Delta S^\ddagger{}_d = +6.1$ (3) cal deg^{-1} mol^{-1}; $\Delta H^\ddagger{}_{CO} - \Delta H^\ddagger{}_{Si} = 0.5$ (1.2) kcal mol^{-1}; $\Delta S^\ddagger{}_{CO} - \Delta S^\ddagger{}_{Si} = -1$ (4) cal deg^{-1} mol^{-1}.

Figure 7. Graph of $\ln (k_d/T)$ vs $1/T$ for $HSiEt_3$.

Time (s)

Figure 5. (a) Absorbance vs time at 420 nm, following the flash of a $Cr(CO)_6/HSiEt_3$/hexane ([$HSiEt_3$] = 10.1 mM) solution under Ar at 25.0 °C. The data are fitted as a second-order reaction. The inset shows a plot of (absorbance)$^{-1}$ vs t. (b) Absorbance vs time at 420 nm, following the flash of a $Cr(CO)_6/HSiEt_3$/hexane ([$HSiEt_3$] = 9.72 mM) solution under CO at 25.0 °C. The data are fitted as a first-order reaction. The inset shows a plot of $\ln (A_t - A_\infty)$ vs t.

[HSiEt₃] (×10⁻² M)
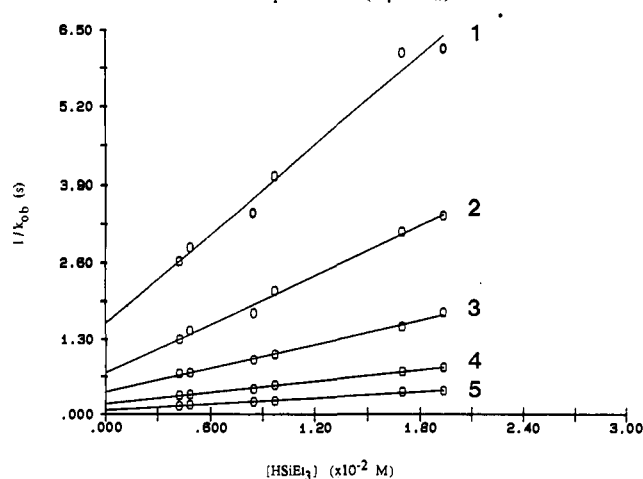
Figure 6. Plots of $1/k_{ob}$ vs [$HSiEt_3$] for $HSiEt_3$-elimination reactions observed after flash photolysis of solutions of $Cr(CO)_6/HSiEt_3$/hexane under 1 atm of CO: (1) 13.2 °C; (2) 18.8 °C; (3) 25.0 °C; (4) 31.8 °C; (5) 39.6 °C.

The rate behavior observed for the reaction of $Cr(CO)_5(HSiEt_3)$ with CO indicates that the reaction involves both $HSiEt_3$ dissociation and recombination steps. However, the nature of the intermediate species is ambiguous, since $Cr(CO)_5$ or $Cr(CO)_5$-(hexane) or both can be steady-state intermediates involved in the overall reaction. Assuming that displacement of hexane by CO or $HSiEt_3$ takes place predominantly via a dissociative pathway, the mechanism is as outlined in eq 5.

$$Cr(CO)_5(HSiR_3) \underset{k_{Si}[HSiR_3]}{\overset{k_d}{\rightleftharpoons}} [Cr(CO)_5] \xrightarrow{k_{CO}[CO]} Cr(CO)_6 \quad (5)$$
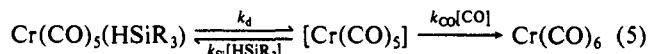
Assuming a steady-state concentration of $Cr(CO)_5$, the rate law obeys eq 6. Upon rearrangement we obtain eq 7. Comparison of eq 7 with eq 4 yields $a = 1/k_d$ and $b = k_{Si}/(k_d k_{CO}$-[CO]). Note that when [CO] is constant, b is constant.

$$k_{ob} = \frac{k_d k_{CO}[CO]}{k_{CO}[CO] + k_{Si}[HSiR_3]} \quad (6)$$

$$1/k_{ob} = 1/k_d + \{k_{Si}/(k_d k_{CO}[CO])\}[HSiEt_3] \quad (7)$$

The rate constants k_d for $HSiR_3$ (R = Et, Ph) dissociation, as determined from the intercepts of the plots of $1/k_{ob}$ vs [$HSiR_3$], from flash photolyses at various temperatures, are listed in Table II. A graph of $\ln (k_d/T)$ vs $1/T$ is shown in Figure 7 for $HSiEt_3$. The corresponding activation parameters are listed as footnotes to Table II. Table II also lists the "competition ratios", the ratios of rate constants for binding to [$Cr(CO)_5$] by CO and $HSiR_3$, respectively. The competition ratios are not far from unity and are nearly independent of temperature; $\Delta H^\ddagger{}_{CO} - \Delta H^\ddagger{}_{Si} = 2$ (1) kcal mol^{-1} for $HSiEt_3$ and $\Delta H^\ddagger{}_{CO} - \Delta H^\ddagger{}_{Si} = 0.5$ (1.2) kcal mol^{-1} for $HSiPh_3$. These observations support the assumption that the intermediate is $Cr(CO)_5$, which reacts with nucleophiles at or near

Photochemical Reactions of Silanes with Cr(CO)6
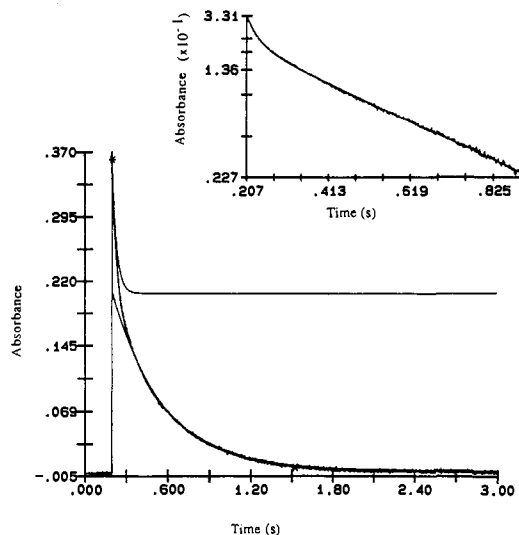
J. Am. Chem. Soc., Vol. 113, No. 18, 1991 6913

Figure 8. Absorbance vs time fitted as a sum of two exponential functions on data obtained at 420 nm, after flash photolysis of a $Cr(CO)_6/$ $HSiClMe_2/$hexane solution ($[HSiClMe_2]$ = 52.1 mM) under 1 atm of CO at 25.0 °C. The inset shows a plot of ln $(A_t - A_\infty)$ vs t.
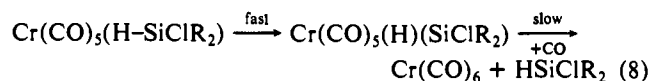
diffusion-controlled rates. The entropies of activation, $\Delta S^\ddagger_d$ = +11 (2) cal deg^{-1} mol^{-1} for HSiEt$_3$ and $\Delta S^\ddagger_d$ = +6.1 (3.0) cal deg^{-1} mol^{-1} for HSiPh$_3$, are moderately positive, which also is consistent with a dissociative mechanism for silane elimination.

The enthalpies of activation for silane dissociation, $\Delta H^\ddagger_d$ = 20.0 (0.5) kcal mol^{-1} for HSiEt$_3$ and $\Delta H^\ddagger_d$ = 16.4 (0.9) kcal mol^{-1} for HSiPh$_3$, should be measures of the upper limits of the corresponding $(CO)_5Cr-(H-SiR_3)$ bond dissociation energies. The value $\Delta H^\ddagger_d$ = 20.0 (0.5) kcal mol^{-1} for $(CO)_5Cr-(H-SiEt_3)$ is very close to the value 21 (2) kcal mol^{-1} obtained from photoacoustic calorimetry measurements.[11]

It is noteworthy that the lower value of $\Delta H^\ddagger_d$ for HSiPh$_3$ as compared with HSiEt$_3$ is just the reverse of the trend observed in $(\eta^5\text{-}C_5H_5)(OC)_2Mn(H)SiR_3$ and $(\eta^6\text{-}C_6H_6)(OC)_2Cr(H)SiR_3$ complexes, in which the more electron-withdrawing substituents on the silicon are found to strengthen the $M-(H-SiR_3)$ bond as the bond form is shifted toward oxidative addition, $M(H)(SiR_3)$. To investigate these effects further, rate constants for silane dissociation from $Cr(CO)_5$ were determined for a series of silanes with a wide range of electronic and steric properties.

$Cr(CO)_5(H-SiClR_2)$ and $Cr(CO)_5(Cl-SiHR_2)$ Complexes. Unlike the cases of HSiEt$_3$, HSiPh$_3$, and other hydridoalkylsilanes, *two* first-order kinetics processes were observed on the millisecond and second time scales in the silane-elimination reactions of HSiClR$_2$ (R = Me, Ph). The data yielded two observed rate constants, $k_{ob(1)}$ for the long-time portion and $k_{ob(2)}$ for the short-time portion of the absorption decay (Table III). Figure 8 displays a plot of absorbance vs time fitted by a sum of two exponential functions on data obtained after flash photolysis of a hexane solution of $Cr(CO)_6$, with $[HSiClMe_2]$ = 52.1 mM, under 1 atm of CO. The graph of ln $(A_t - A_\infty)$ vs time, shown in the inset, also indicates two distinct processes.

The observed kinetics behavior implies that two reaction species exist at comparable concentrations in the time domain under study. The question arises as to whether the two species are generated consecutively or simultaneously from the $Cr(CO)_5$(hexane) precursor. Among the reaction schemes that might be considered to account for the observed kinetics, two are worthy of special attention. The first, described in eq 8, assumes that the two species

$$Cr(CO)_5(H-SiClR_2) \xrightarrow{\text{fast}} Cr(CO)_5(H)(SiClR_2) \xrightarrow[+CO]{\text{slow}}$$
$$Cr(CO)_6 + HSiClR_2 \quad (8)$$

involved are the adduct $Cr(CO)_5(H-SiClR_2)$ and the oxidative addition product $Cr(CO)_5(H)(SiClR_2)$. The latter complex is presumably produced from the former via intramolecular oxidative addition in the faster of the two steps observed. An analogous
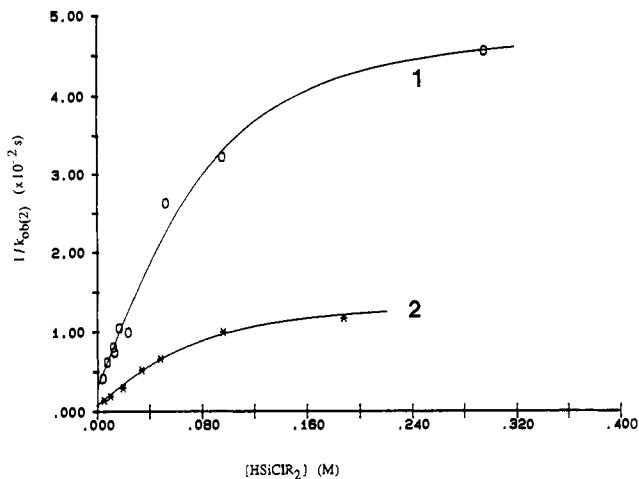

Figure 9. Plots of $1/k_{ob(2)}$ vs $[HSiClR_2]$ for data obtained after flash photolysis of $Cr(CO)_6/HSiClR_2/$hexane solutions under CO at 25.0 °C. R = Me (1), Ph (2).

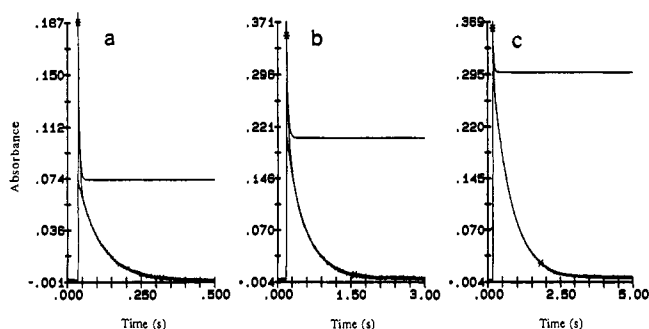**Figure 10.** Absorbance vs time at 420 nm, following flash photolysis of $Cr(CO)_6/HSiClMe_2/$hexane solutions under CO at 25.0 °C. $[HSiClMe_2]$ = 3.93 (a), 52.1 (b), 95.2 mM (c). The data were fitted as a sum of two exponential functions.

two-stage reaction involving H–C bond activation has been observed.[18] In this model, the observed fast process corresponds to oxidative addition and the slower to the reductive elimination step.

A second possible reaction scheme involves interconversion of two $Cr(CO)_5$(silane) complexes. The hydridochlorosilane can interact with $Cr(CO)_5$ via the σ electrons in the H–Si bond to form $Cr(CO)_5(H-SiClR_2)$ or via the chlorine atom or Cl–Si bond to form $Cr(CO)_5(Cl-SiHR_2)$. The notation $(Cl-SiHR_2)$ implies that the interaction may occur via donation of a lone pair on Cl to the metal or through a three-center, two-electron interaction such as that observed for the $Cr-(H-Si)$ bond. As shown in eq 9, the two complexes can each undergo substitution by CO to regenerate $Cr(CO)_6$.

$$\tag{9}$$
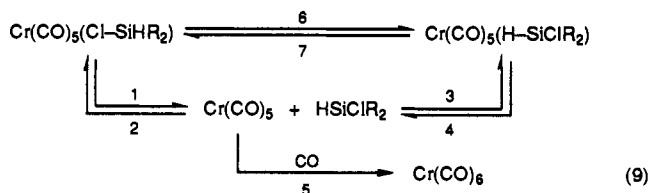
The experimentally determined rate constants for both steps were found to depend on $[HSiClR_2]$. Plots of $1/k_{ob(1)}$ vs $[HSiClR_2]$ are linear over a wide concentration range (4×10^{-3} to 0.4 M), while plots of $1/k_{ob(2)}$ vs $[HSiClR_2]$ are curved at high concentrations, as shown in Figure 9. Furthermore, the relative magnitudes of the absorbance changes in the decay signal vary with the HSiClR$_2$ concentration, as shown in Figure 10. The experimental results are inconsistent with the reaction scheme
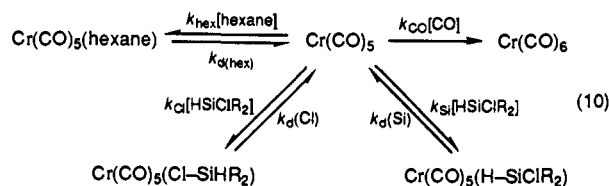
(18) Weiller, B. H.; Wasserman, E. P.; Bergman, R. G.; Moore, C. B.; Pimentel, G. C. *J. Am. Chem. Soc.* **1989**, *111*, 8288–8290.

Table III. Rate Constants of Reactions Observed after Flash Photolysis of $Cr(CO)_6$ in Hexane in the Presence of Chlorinated Silanes at 25.0 °C under 1 atm of CO

silane	[silane], mM	$k_{ob(1)}$, s^{-1}	$10^{-2}k_{ob(2)}$, s^{-1}
HSiClMe$_2$	3.95	11.3 (0.5)	2.4 (0.1)
	7.32	10.6 (1.9)	1.6 (0.2)
	12.1	9.0 (2.1)	1.2 (0.1)
	13.1	8.2 (1.7)	1.3 (0.1)
			0.19 (0.02)^a
	16.8	6.9 (0.5)	1.0 (0.1)
	23.5	7.1 (1.5)	1.0 (0.2)
	52.1	3.4 (0.8)	0.38 (0.08)
			0.23 (0.02)^a
	95.2	1.7 (0.1)	0.31 (0.02)
	296	0.92 (0.05)	0.22 (0.03)
HSiClPh$_2$	4.88	76 (7)	7.0 (0.7)
	9.74	61 (3)	5.1 (0.2)
	19.4	45 (1)	3.31 (0.05)
	33.9	36 (3)	1.9 (0.1)
	48.3	29 (5)	1.5 (0.3)
			0.97 (0.02)^a
	95.8	21 (2)	1.0 (0.1)
			0.73 (0.22)^a
	188	13 (8)	0.85 (0.08)
	445	6.0 (0.4)	
ClSiMe$_3$	11.4		1.08 (0.06)
ClSiMePh$_2$	90.6		2.9 (0.2)
HSiCl$_3$	450	1.2 (0.1) × 10^3	
HSiCl$_2$Ph	190	2.1 (0.1) × 10^2	

^{a} Obtained from flash photolysis of the same solutions under Ar instead of CO.

shown in eq 8, which predicts that the rate of the faster step should be independent of [HSiClR$_2$]. The results are consistent with concurrent formation of two distinct species that interconvert on a time scale comparable to that for reaction with CO. The fact that varying [HSiClR$_2$] affects the relative amounts of the two intermediates, coupled with the observation of two distinct decay processes, in turn suggests that interconversion occurs through a dissociative process (steps 1–4, eq 9), rather than through an intramolecular, kinetically unimolecular pathway (steps 6 and 7, eq 9). Thus the kinetics data are consistent with the reaction model outlined in eq 10. It should be noted that this mechanism invokes

$$Cr(CO)_5(hexane) \underset{k_{-d(hex)}}{\overset{k_{hex}[hexane]}{\rightleftharpoons}} Cr(CO)_5 \overset{k_{CO}[CO]}{\longrightarrow} Cr(CO)_6$$

$$k_{Cl}[HSiClR_2] \diagdown \diagup k_{-d(Cl)} \quad k_{-d(Si)} \diagdown \diagup k_{Si}[HSiClR_2] \quad (10)$$

$$Cr(CO)_5(Cl-SiHR_2) \qquad\qquad Cr(CO)_5(H-SiClR_2)$$

the assumption that displacement of hexane by CO or silane takes place predominantly via a dissociative pathway. $Cr(CO)_5$(hexane) exists in a steady-state concentration on the time scale of silane elimination (>ms) under the reaction conditions employed.

To distinguish the two possible species, $Cr(CO)_5(Cl-SiHR_2)$ and $Cr(CO)_5(H-SiClR_2)$, flash photolysis of hexane solutions of $Cr(CO)_6/MeSiClR_2$ (R = Me, Ph) under 1 atm of CO were also investigated. For MeSiClR$_2$, only a Cl–SiR$_3$ interaction with $Cr(CO)_5$ is possible. Figure 11 displays the signal obtained from flash photolysis of a hexane solution of $Cr(CO)_6$ with [ClSiMe$_3$] = 11.4 mM. The decay clearly obeys simple first-order kinetics. The rate constant, k_{ob} = 1.1 × 10^2 s^{-1}, is very close to the rate constant obtained from the fast portion of the signal for HSiClMe$_2$ at a similar concentration ([HSiClMe$_2$] = 12.1 mM, $k_{ob(2)}$ = 1.2 × 10^2 s^{-1}). The time-resolved spectrum for $Cr(CO)_5(Cl-SiMe_3)$, in which ClSiMe$_3$ is presumably bound to Cr via the chlorine atom or Si–Cl bond, exhibits $\lambda_{max} \approx$ 460 nm (Figure 12, curve 3). The time-resolved spectra obtained from flash photolysis of a hexane solution of $Cr(CO)_6$, with [HSiClMe$_2$] = 95.2 mM, under 1 atm of CO, are also shown in Figure 12. Spectrum 1 arises from the longer lived component of the absorbance change and shows $\lambda_{max} \approx$ 410 nm. Spectrum 2, which comes from the faster portion of the absorbance change, exhibits $\lambda_{max} \approx$ 450 nm. The absorption

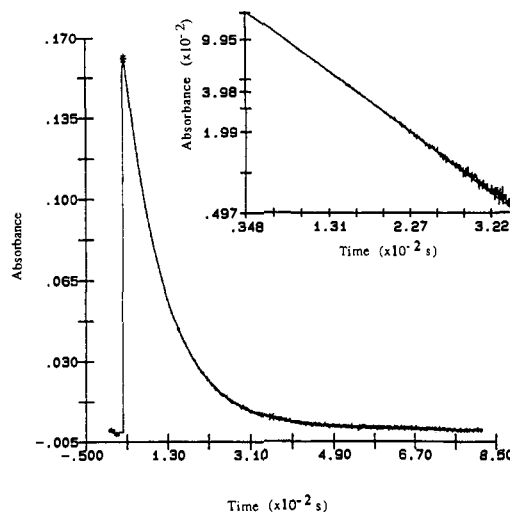**Figure 11.** Absorbance vs t and ln $(A_t - A_\infty)$ vs t (inset) at 460 nm after flash photolysis of a solution of $Cr(CO)_6/ClSiMe_3/hexane$ ([ClSiMe$_3$] = 11.4 mM) under CO at 25.0 °C.

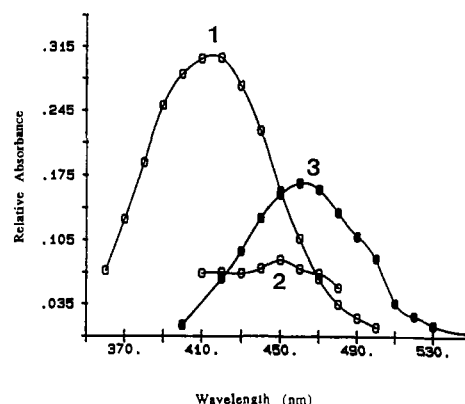**Figure 12.** Transient spectra obtained from flash photolysis of a $Cr(CO)_6/HSiClMe_2/hexane$ solution ([HSiClMe$_2$] = 95.2 mM, spectra 1 and 2; see text) and a solution of $Cr(CO)_6/ClSiMe_3/hexane$ ([ClSiMe$_3$] = 11.4 mM, spectrum 3) under CO at 25.0 °C.
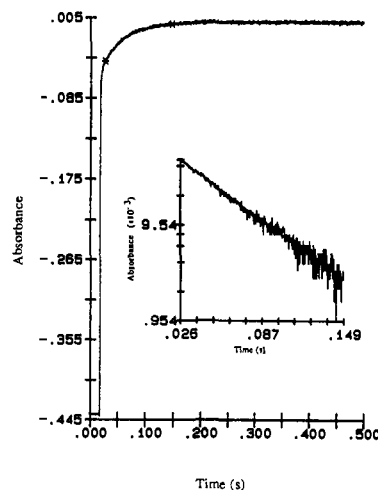
Figure 13. Absorbance vs t and ln $(A_\infty - A_t)$ vs t (inset) at 420 nm after flash photolysis of a solution of $Cr(CO)_6/HSiClMe_2/hexane$ ([HSiClMe$_2$] = 52.1 mM) under Ar at 25.0 °C.

maximum for this shorter lived component lies quite near that for $Cr(CO)_5(Cl-SiMe_3)$. Similar observations were made with respect to the HSiClPh$_2$ and MeSiClPh$_2$ complexes. Thus, it is reasonable to assign $Cr(CO)_5(Cl-SiHR_2)$ as the rapidly decaying, less stable species.

When a $Cr(CO)_6/HSiClMe_2/hexane$ solution ([HSiClMe$_2$] = 52.1 mM) is flash-photolyzed under Ar instead of under CO,

an exponential growth signal is observed at 420 nm. The rate constant derived from this transient, 23 s^{-1}, is very close to 22 s^{-1}, the $k_{ob(2)}$ value obtained from solutions at the highest [HSiClMe$_2$] concentrations under CO (Table III). This observation is consistent with conversion of the less stable complex Cr(CO)$_5$(Cl–SiHR$_2$) ($\lambda_{max} \approx 450$ nm) to the more stable complex Cr(CO)$_5$-(H–SiClR$_2$) ($\lambda_{max} \approx 410$ nm) after the initial formation of the two intermediates. At low silane concentration in the presence of added CO, the two intermediates (silane adducts) decay and the Cr(CO)$_5$ formed is scavenged by CO before further reaction with silane can provide a means to interconvert the two intermediates. A high silane concentration or in the absence of added CO, after the silane dissociates, Cr(CO)$_5$ can be recaptured by silane before CO scavenges it, thus providing a mechanism for interconversion and hence equilibration between intermediates. So high silane concentration provides thermodynamic control and favors more Cr(CO)$_5$(H–SiClR$_2$) adduct; low silane concentration presumably results in kinetic control and favors the Cr(CO)$_5$-(Cl–SiHR$_2$) adduct, consistent with Figure 10. It also further supports the idea that interconversion of the two species occurs via dissociative pathways (eq 10).

Since no simple overall reaction rate law expression can be derived for the reaction, computer simulations of the reaction scheme (eq 10) were carried out. Simulations employing the numerical integration program, HAVCHM,[19] or employing rate law expressions based on the assumption of steady-state concentrations of Cr(CO)$_5$ confirmed that the transient absorbance should vary in time as the sum of two exponential terms, in agreement with the experimental results (supplementary material).

The simulation calculations show that $k_{simu(1)}$ and $k_{simu(2)}$ approach the assumed $k_{d(Si)}$ and $k_{d(Cl)}$ values, respectively when [HSiClR$_2$] approaches zero. The calculations also confirmed that at very high HSiClR$_2$ concentrations, $k_{ob(2)}$ should approach a constant value $k'_{ob(2)}$ (eq 11) (supplementary material), which is

$$k'_{ob(2)} = (k_{d(Cl)}k_{Si} + k_{d(Si)}k_{Cl})/(k_{Si} + k_{Cl}) \qquad (11)$$

close to the apparent rate constant for the approach of Cr-(CO)$_5$(Cl–SiHR$_2$) and Cr(CO)$_5$(H–SiClR$_2$) to equilibrium in the absence of added CO, before they eventually form the final product Cr(CO)$_6$.

The dissociative mechanism for Cr(CO)$_5$(H–SiClR$_2$) and Cr(CO)$_5$(Cl–SiHR$_2$) interconversion is consistent with the trajectories of the reactions of silanes[20a–c] or hydrocarbons[20d,e] with metal centers proposed from structure correlations[20a–d] and molecular orbital calculations.[20e] It was proposed that H–CR$_3$ or H–SiR$_3$ approaches the metal in a manner in which the hydrogen atom lies collinearly with metal and C or metal and Si atoms. According to the *principle of microscopic reversibility*, the thermal elimination of H–SiR$_3$ must traverse the same reaction surface in the reverse direction. Thus one can envision that the interconversion of Cr(CO)$_5$(H–SiClR$_2$) and Cr(CO)$_5$(Cl–SiHR$_2$) is unlikely to proceed via a pathway in which there is significant bonding with Cr(CO)$_5$ in the transition state.

Flash photolysis of hexane solutions of Cr(CO)$_6$ and HSiCl$_3$ or HSiCl$_2$Ph under CO afforded signals with only one exponential decay in the millisecond and second time scales. The time-resolved spectra show absorbance bands with λ_{max} shorter than 410 nm. Both the values for the rate constants and the values of λ_{max} indicate that the transients are due to Cr(CO)$_5$(H–SiCl$_3$) and Cr(CO)$_5$(H–SiCl$_2$Ph) complexes (Table III). Given that the identified chlorine-coordinated complexes are less stable than the corresponding H–Si-coordinated complexes, it is reasonable that the Cl-coordinated species for HSiCl$_3$ and HSiCl$_2$Ph should decay

(19) (a) Stabler, R. N.; Chesick, J. P. *Int. J. Chem. Kinet.* **1978**, *10*, 461. (b) Chesick, J. P. *J. Chem. Educ.* **1988**, *65*, 599.
(20) (a) Burgi, H. B. *Angew. Chem., Int. Ed. Engl.* **1975**, *14*, 460. (b) Schubert, U.; Schloz, G.; Muller, J.; Ackermann, K.; Worle, B.; Stansfield, R. F. D. *J. Organomet. Chem.* **1986**, *306*, 303. (c) Schubert, U.; Ackermann, K.; Kraft, G.; Worle, B. *Z. Naturforsch. B: Anorg. Chem., Org. Chem.* **1983**, *38*, 1488. (d) Crabtree, R. H.; Holt, E. M.; Lavin, M.; Morehouse, S. M. *Inorg. Chem.* **1985**, *24*, 1986. (e) Saillard, J. Y.; Hoffmann, R. *J. Am. Chem. Soc.* **1984**, *106*, 2006.

Table IV. Rate Constants of Reactions Observed in Silane-Elimination Reactions at 25.0 °C and Tolman's Electronic Parameter and Cone Angle for Corresponding Phosphine Compounds

silane[a]	k_d, s^{-1}	k_{CO}/k_{Si}	ν, cm^{-1}	θ, deg[f]
HSiEt$_3$	2.6 (0.2)	0.41 (0.04)	2061.9	132
HSiMe(Cy)$_2$	3.1 (0.5)	0.38 (0.09)	2058.9	(153)
HSiPhMe$_2$	6.7 (0.7)	0.33 (0.04)	2065.3	122
H$_2$SiPh$_2$	15.4 (1.5)	0.25 (0.03)	2073.3	128
HSiClMe$_2$	15.8 (1.7)	[1.1]^b	2076.1	(120)
HSiMePh$_2$	21 (4)	0.26 (0.06)	2067.0	136
HSi(i-Pr)$_3$	23 (2)	0.41 (0.06)	2059.2	160
HSiClPh$_2$	86 (4)	[1.8]^b	2080.7	(138)
HSi(CH$_2$Ph)$_3$	95 (8)	0.47 (0.06)	2066.4	165
HSiPh$_3$	143 (9)	0.26 (0.02)	2068.9	145
HSi(C$_6$F$_5$)Me$_2$	148 (10)	0.74 (0.07)	2072.5	(140)
HSiFPh$_2$	365 (52)	0.32 (0.06)	2082.9	(131)
HSiPhCl$_2$	2200^e	[2.0]^c	2092.1	(131)
HSiCl$_3$	12000^e	[5.0]^d	2097.0	124
HSi(C$_6$F$_5$)$_3$	$\gg$12000		2090.9	184

^{a} [silane] = 3–32 mM. ^{b} Estimated from plots of $1/k_{ob(1)}$ vs [HSiClR$_2$] (R = Me, Ph) for data in the range of [HSiClR$_2$] < 55 mM. ^{c} Estimated according to values of the other silanes. ^{d} Estimated according to k_{CO}/k_{Si} for HSiEt$_3$ and the relative rate constant (k, Table I) for hexane displacement by HSiEt$_3$ and by HSiCl$_3$, assuming a dissociative mechanism. ^{e} Calculated according to eq 6, $k_{ob(1)}$ (Table III), and k_{CO}/k_{Si}. ^{f} The cone angle values in parentheses for PR$_2$R' were calculated from those of PR$_3$ and PR'$_3$: $\theta_{PR_2R'} = (2/3)\theta_{PR_3} + (1/3)\theta_{PR'_3}$.
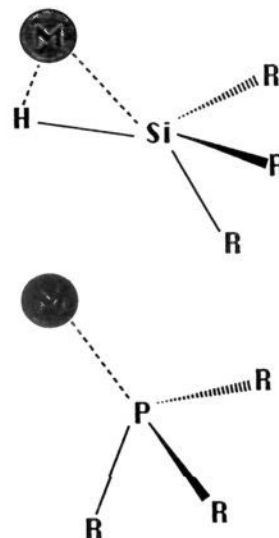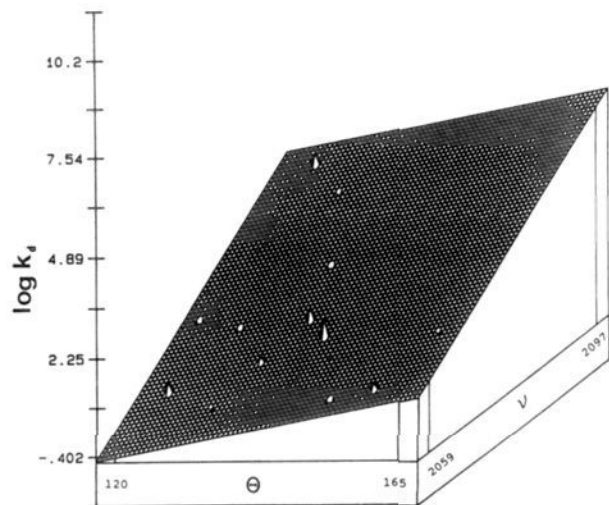

Figure 14. Schematic models of HSiR$_3$ and PR$_3$ bonding to a metal center.

much more rapidly than the observed transients, even if they were formed in significant amounts. When a solution of Cr(CO)$_6$ with 0.47 M MeSiCl$_3$ was flash-photolyzed under 1 atm of CO, a transient signal due to Cr(CO)$_5$(MeSiCl$_3$) was not observed on the millisecond or second time scales.

Substituent Effects. Silane dissociation rate constants (k_d) from Cr(CO)$_5$(HSiR$_2$R') for a series of hydridosilanes with a wide range of electronic and steric properties were examined. As in the case of HSiR$_3$ (R = Et, Ph), k_d and k_{CO}/k_{Si} values were calculated from the intercepts and the slopes of plots of $1/k_{ob}$ vs [HSiR$_2$R'], analogous to those shown in Figure 6. The values are collected in Table IV. Efforts to determine the rate constant for dissociation of HSi(C$_6$F$_5$)$_3$ from Cr(CO)$_5$[HSi(C$_6$F$_5$)$_3$] were, however, not successful.

The silane dissociation rate constants, k_d, vary over almost 4 orders of magnitude in the series of silanes investigated. The most immediately obvious feature of the overall trend is that the dissociation rates are largest for the silanes with the most electron-withdrawing groups attached. To obtain a more formal sense of the dependencies on electronic and steric properties of the silane, we consider the bound silane as roughly isoelectronic with the

Figure 15. Linear free energy relationship for reductive elimination of silanes from $Cr(CO)_5$, eq 12.

corresponding phosphorus ligand, as illustrated in Figure 14. Here the H–Si bond is analogous to the phosphorus lone pair, and the $SiR'R_2$ group is analogous to the corresponding $PR'R_2$. Giering and co-workers have adopted a similar approach,[21a] in which they transferred stereoelectronic parameters of PR_3 to SiR_3 substituents to evaluate the electronic and steric factors influencing the addition of the (*p*-anisylphenyl)carbenium ion to allylsilanes. To test the electronic and steric influences, we employ a three-parameter multivariate regression, eq 12, in which log k_d is related to the

$$\log k_d^i = a\nu_i + b\theta_i + c \qquad (12)$$

Tolman cone angle, θ, of $PR'R_2$ and to the totally symmetric CO stretching frequency of $(CO)_3Ni(PR'R_2)$, ν, which measures the donor–acceptor character of $PR'R_2$.[21b] The relevant values are listed in Table IV. Despite the assumptions and approximations made, a fairly good linear relationship, log $k_d = 9.8 \times 10^{-2}\nu + 3.3 \times 10^{-2}\theta - 2.1 \times 10^2$, with correlation coefficient $R = 0.95$, is found. The coefficients of the electronic and steric terms show that the dissociation reaction is promoted as the groups on Si are more electron-withdrawing (increasing ν) or larger (increasing θ). Figure 15 shows a plot of the surface described by eq 12 and the experimental points in relation to the calculated surface. From the slopes along the ν and θ axes, it can be seen that the variation in the electronic term accounts for about 70% of the variation in log k_d for the group of ligands studied.

It is not surprising that the dissociation of $HSi(C_6F_5)_3$ is too fast to measure, if indeed the complex is formed at all. A very high value for k_d is predicted from the electronic and steric parameters for $P(C_6F_5)_3$.

In summary, the two results of most significance arising from this work are as follows: (a) Silanes containing both H–Si and Cl–Si bonds may bond to $Cr(CO)_5$ through either the H–Si or

Cl–Si bonds. For the former, the two-electron, three-center character of the bonding is established by analogy with much studied adducts such as $(\eta^5\text{-}C_5H_5)(OC)_2Mn(H)SiR_3$ or $(\eta^6\text{-}C_6H_6)(OC)_2Cr(H)SiR_3$. For the latter, which generally exhibit weaker bonding than H–Si bonding, it is not clear whether the interaction with Cr occurs through a Cl lone pair or through the Cl–Si bond, in a manner analogous to H–Si bonding, given that examples of Cl–Si oxidative addition to metal centers are known.[22] Interconversion of the H–Si and Cl–Si bonding forms occurs through dissociation of the ligand rather than by some lower free energy nondissociative pathway. (b) The interactions of silane with $Cr(CO)_5$ are clearly weaker than in $(\eta^5\text{-}C_5H_5)(OC)_2Mn(H)SiR_3$ or $(\eta^6\text{-}C_6H_6)(OC)_2Cr(H)SiR_3$, suggesting that weakening of the Si–H bond in the $Cr(CO)_5$ complexes is less advanced. The stability of H–Si complexes decreases as the groups on silane are more electron-withdrawing. This result is just the opposite of the trend seen in all other H–Si complexes of which we are aware.[3,6,7] It raises interesting questions regarding the nature of the bond. In $(\eta^5\text{-}C_5H_5)(OC)_2Mn(H)SiR_3$ and related complexes, the presence of electron-withdrawing groups on Si is deemed to stabilize the complex through the stronger bonding interaction between a metal d orbital and the σ^* orbital of the Si–H bond.[3,6] In the $Cr(CO)_5$ complexes, the energy levels of the d orbitals of appropriate symmetry are presumably much lower; Cr in $Cr(CO)_5$ is a strongly electrophilic center. Back-bonding into the silane σ^* orbital is thus a less important component of the bonding. Whatever increase in such bonding might occur as the groups on Si become more electron-withdrawing, it fails to offset the concurrent weakening in the σ bond between H–Si and Cr, which is the principal component of the bonding in these complexes.

Supplementary Material Available: A table of rate constants for $HSiEt_3$ and $HSiPh_3$ elimination from $Cr(CO)_5$ in hexane at various temperatures under 1 atm of CO, a table of rate constants for silane elimination reactions observed after flash photolysis in hexane in the presence of silanes at 25.0 °C under 1 atm of CO, text, tables, and figures describing the results of HAVCHEM simulations, and the derivation of the rate law expressions (eq 10) (13 pages). Ordering information is given on any current masthead page.

(21) (a) Panek, J. S.; Prock, A.; Eriks, K.; Giering, W. P. *Organometallics* **1990**, *9*, 2175. (b) Tolman, C. A. *Chem. Rev.* **1977**, *77*, 313.

(22) (a) Uson, R.; Oro, L. A.; Fernandez, M. J. *J. Organomet. Chem.* **1980**, *193*, 127. (b) Uson, R.; Oro, L. A.; Ciriano, M. A.; Gonzalez, R. *J. Organomet. Chem.* **1981**, *205*, 259. (c) Yamashita, H.; Hayashi, T.; Kobayashi, T.-a.; Tanaka, M.; Goto, M. *J. Am. Chem. Soc.* **1988**, *110*, 4417. (d) Zlota, A. A.; Frolow, F.; Milstein, D. *J. Chem. Soc., Chem. Commun.* **1989**, 1826. (e) Yamashita, H.; Kawamoto, A. M.; Tanaka, M.; Goto, M. *Chem. Lett.* **1990**, 2107.